Magnesium

Proceedings of the 7th International Conference on
Magnesium Alloys and Their Applications

Edited by
K. U. Kainer

DGM

WILEY-VCH Verlag GmbH & Co. KGaA

Editor:
Prof. Dr. K. U. Kainer
GKSS-forschungszentrum
Institut für Werkstofforschung
Max-Planck-Straße
21502 Geesthacht
Germany

7th International Conference on Magnesium Alloys and Their Applications

from 06-09 November 2006 in Dresden
Organized byDGM (Deutsche Gesellschaft für Materialkunde e. V.)

Library of Congress Card No.: applied for

British Library Cataloguing-in-Publication Data:
A catalogue record for this book is aailable from the British Library

Bibliografic information published by the Deutsche Nationalbibliothek
The Deutsche Nationalbibliothek lists this publication in the Deutsche Nationalbibliografie; detailed bibliografic data is available in the Internet at <http://dnb.d-nb.de>.

Printed on acid-free paper

Printed in the Federal Republic of Germany

Composition: W.G.V. Verlagsdienstleistungen GmbH, Weinheim
Printing: betz-Druck GmbH, Darmstadt
Bookbinding: Litges & Dopf Buchbinderei GmbH, Heppenheim

ISBN: 978-3-527-31764-6

Microstructure and Thermal Stability of Ultra Fine Grained Mg-4Tb-2Nd Alloy Prepared by High Pressure Torsion

J. Cizek, I. Prochazka, B. Smola, I. Stulikova, M. Vlach
Faculty of Mathematics and Physics, Charles University, Prague, Czech Republic
R. K. Islamgaliev, O. Kulyasova
Institute of Physics of Advanced Materials, Ufa State Aviation Technical University, Ufa, Russia

1 Introduction

Low density Mg-based alloys allow for a significant weight reduction which rises the effectiveness in a broad range of industrial applications. Unfortunately, the use of most of Mg alloys is limited to low temperature applications due to degradation of their mechanical properties at temperatures above 200 °C. There are several approaches how to overcome this problem. The particularly promising way is the use of non-traditional rare earth alloying elements [1]. The Mg-Tb-Nd ternary alloy represents a novel age hardenable Mg-based alloy with enhanced strength and favorable creep properties even at elevated temperatures [2]. The supersaturated solid solution of Tb in Mg decomposes in the following sequence of consequently precipitating phases: α'(hcp) $\rightarrow$ β"(D019) $\rightarrow$ β_1(fcc) $\rightarrow$ β(cubic) [2]. Despite the favorable strength and thermal stability, a disadvantage of this alloy consists in a poor ductility insufficient for most of the potential industrial applications. Grain refinement is a well-known method how to improve ductility of metallic materials. An extreme grain size reduction is achieved by severe plastic deformation (SPD), see [3] for review. The methods based on SPD produce bulk materials with ultra fine grain (UFG) structure. The largest grain refinement is achieved by high pressure torsion (HPT) [3]. The HPT technique has been already successfully employed for preparation of UFG Mg10%Gd alloy with grain size $\approx$ 100 nm [4]. Small grain size, which lies in the nanocrystalline range, leads to a significant volume fraction of grain boundaries which represent obstacles for movement of dislocations. It causes a significant hardening of UFG metals in addition to the age hardening effect caused by fine precipitates. As a consequence, the UFG metals exhibit a favorable combination of very high strength and a reasonable ductility.

The aim of this work is microstructure characterization of Mg-Tb-Nd alloy prepared by HPT and its comparison with the microstructure of corresponding coarse grained material. Subsequently, we compared the precipitation sequence in the UFG sample and the coarse grained alloy. A typical feature of UFG structure is very high number of lattice defects introduced by SPD. Obviously, defects introduced by SPD play crucial role in the UFG structure. Detailed characterization of these defects represents, therefore, an important task in microstructure investigations of the UFG materials. For this reason we employed positron lifetime (PL) spectroscopy in the present work. PL spectroscopy represents a well established non-destructive technique with very high sensitivity to open-volume defects like vacancies, dislocations, etc. [5]. Thus, PL spectroscopy is an ideal tool for defects studies of UFG materials. PL spectroscopy was combined with transmission electron microscopy (TEM), electrical resisitivity and microhardness investigations.

2 Experimental

Specimens of technically pure Mg (99.9 %) and Mg-4%Tb-2%Nd (Mg4Tb2Nd) alloy were investigated. The Mg4Tb2Nd alloy was prepared by squeeze casting using the technically pure Mg. The as-cast material was subjected to a solution annealing at 525 °C for 6 hours. This treatment is sufficient to dissolve the alloying elements completely [6]. The solution annealing is finished by quenching into water of room temperature. To fabricate the UFG structure, the as-received Mg and the solution treated Mg4Tb2Nd alloy were deformed by HPT at room temperature using 5 rotations under a high pressure of 6 GPa. After detailed characterization of the as deformed microstructure, the specimens were subjected to step-by-step isochronal annealing (20°C/20 min). Each annealing step was finished by quenching into water of room temperature and subsequent investigations performed at room temperature.

A fast-fast PL spectrometer similar to that described in [7] with time resolution of 160 ps was used in this work. The TEM observations were carried out on a JEOL 2000 FX electron microscope operating at 200 kV. The Vickers microhardness, HV, was measured at a load of 100 g applied for 10 s using a LECO M-400-A hardness tester. Electrical resistivity was measured at 77 K by means of the dc four-point method with a dummy specimen in series. Relative electrical resistivity changes $\Delta\rho/\rho$ were obtained to within an accuracy of 10^{-4}. The effect of a parasitic thermo-electromotive force was suppressed by a change in polarity.

3 Results and Discussion

The positron lifetimes τ_i and the relative intensities I_i of the components resolved in the PL spectra of studied specimens are listed in Table 1. The well annealed Mg reference specimen exhibits a single component PL spectrum with lifetime $\tau_B = 225$ ps which agrees well with the calculated Mg bulk lifetime [8]. Thus, defect density in the reference Mg specimen is negligible and virtually all positrons annihilate from the free state. The as cast Mg4Tb2Nd alloy exhibits two component PL spectrum. The shorter component with lifetime τ_1 comes from free positrons, while the component with a longer lifetime τ_2 represents a contribution of positrons trapped at defects. The lifetime τ_2 agrees well with the lifetime of positrons trapped at dislocations in Mg [8]. Thus, it can be concluded that the as-cast alloy contains dislocations introduced in the course of casting and shaping of the specimens. Dislocation density ρ_D in the specimen can be calculated using the two state trapping model [5]

$$\rho_D = \frac{1}{\nu_D}\frac{I_2}{I_1}\left(\frac{1}{\tau_B} - \frac{1}{\tau_2}\right), \tag{1}$$

where ν_D stands for the positron trapping coefficient for dislocations in Mg. In the present work we use $\nu_D = 1 \cdot 10^{-4}$ m^2 s^{-1} [9]. The Eq. (1) then yields $\rho_D = 8 \cdot 10^{12}$ m^{-2} for the as cast Mg4Tb2Nd.

The solution treated alloy exhibits coarse grains with mean diameter of over 500 μm. One can see from Table 1 that the most of positrons in the solution treated Mg4Tb2Nd annihilate from the free state and contribute to the shorter component. However, there is also a weak component with lifetime $\tau_2 \approx 280$ ps, which is close to the lifetime of positrons trapped at Mg vacancy [8]. It indicates that a small fraction of positrons is trapped in quenched-in vacancies. The free vacancies in Mg are not stable at room temperature, therefore, the observed defects are va-

cancies bound to Tb or Nd atoms. Similar type of defects, i.e. the quenched-in vacancies bound to Gd atoms, were found also in the solution treated Mg-Gd alloy [8]. No contribution of positrons trapped at dislocations was found in the PL spectrum of the solution treated Mg4Tb2Nd. It testifies that dislocations were annealed out under detectable limit (below 10^{12} m^{-2}). This conclusion is supported also by TEM observations. It should be also mentioned that no precipitates were observed by TEM in the solution treated alloy.

Table 1: Positron lifetimes τ_i and relative intensities I_i of the components resolved in the PL spectra

Sample	τ_1 (ps)	I_1 (%)	τ_2 (ps)	I_2 (%)
well annealed Mg (280°C/30min)	224.8 ± 0.5	100	–	–
Mg4Tb2Nd – as cast	193 ± 2	44 ± 2	255 ± 2	66 ± 1
Mg4Tb2Nd – solution treated	220 ± 1	91 ± 1	280 ± 20	9 ± 1
Mg4Tb2Nd – HPT deformed	180 ± 2	14.9 ± 0.4	256 ± 2	85.1 ± 0.4

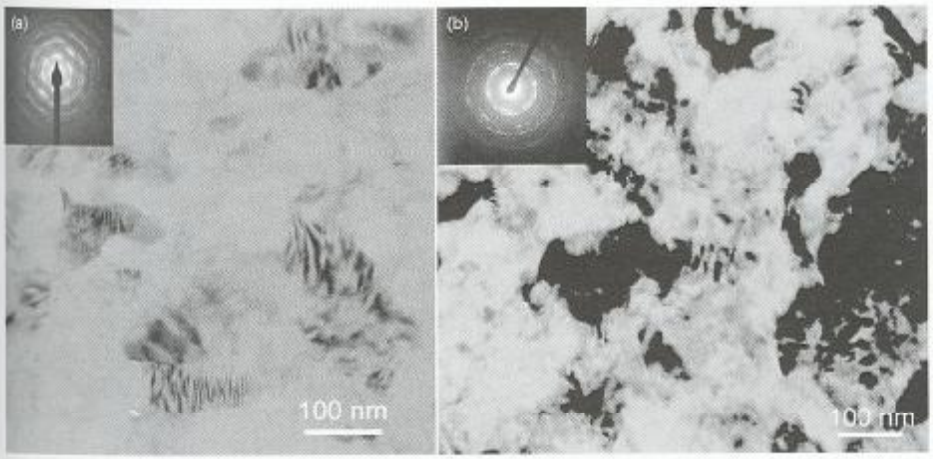

Figure 1: TEM images of UFG Mg4Tb2Nd alloy: (a) as deformed structure, (b) sample annealed up to 140 °C

A representative TEM image of HPT-deformed Mg4Tb2Nd alloy is shown in Fig. 1a. The specimen shows a homogeneous UFG structure with grain size around 100 nm. The dominant component in the PL spectrum exhibits lifetime $\tau_2 \approx 256$ ps which corresponds to positrons trapped at dislocations in Mg. Thus, majority of positrons are trapped at dislocations introduced by SPD. The dislocation density $\rho_D = 3 \cdot 10^{13}$ m^{-2} was calculated using Eq. (1). A high density of dislocations can be see also on the TEM image. It is too high to resolve individual dislocation lines. The dislocations are homogeneously distributed throughout whole grains. The electron diffraction pattern testifies long angle miss-orientation of neighboring grains. The specimen exhibits (00.1) type texture. No precipitates were found in the as-deformed alloy by TEM. The strong grain refinement and a high number of dislocations leads to a substantial hardening which can be seen in a rise of microhardness: the HPT-deformed alloy exhibits about 140 % higher microhardness compared to the solution treated specimen. Temperature dependence of

the intensity of trapped positrons in the solution treated and the HPT-deformed alloy subjected to isochronal annealing are shown in Figs. 2a and 2b, respectively. Temperature dependence of microhardness HV for both the specimens is shown in Figs. 3a,b.

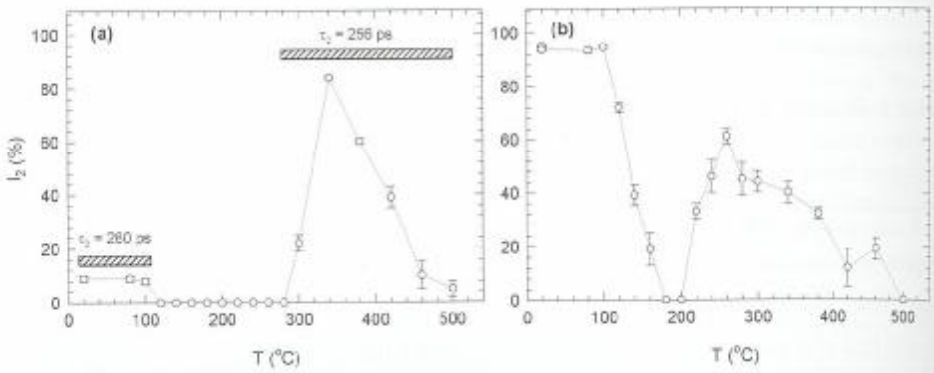

Figure 2: Temperature dependence of the intensity I_2 of positrons trapped at defects: (a) solution treated Mg4Tb2Nd alloy, (b) HPT deformed Mg4Tb2Nd alloy

Let us start to discuss the precipitation effects in the solution treated alloy. The quenched-in vacancies bound to the alloying elements are annealed out by annealing at 120 °C. It is seen in Fig. 2a as disappearance of the long lived component with lifetime $\tau_2 = 280$ ps and intensity I_2. The sample exhibits a single component PL spectrum in the temperature range (120–280) °C, i.e. there are no active positron traps in this temperature interval. From Fig. 3a, it becomes clear that the precipitation of the β" phase particles starts around 80 °C and causes a remarkable hardening. The β' phase particles are fully coherent with the Mg lattice and, thereby, no open volume defects are introduced by precipitation of the β" phase. The positron affinity of the β" phase is not known so far, but our results show clearly that it is most probably not favorable for positrons. As a consequence, there is no positron trapping in the β" precipitates and PL spectroscopy is not sensitive to the precipitation of the β" phase. TEM investigations revealed out that fine spherical β" phase precipitates transform into fine plates in the temperature interval (180–240) °C. One can see in Fig. 3b that it has a strong hardening effect with the peak hardness at 210 °C. Fine β"phase plates precipitates in a triangular configuration parallel with the prismatic planes {11.0}. Further annealing up to 270 °C leads to growth of the plate shaped precipitates (diameter 20–30 nm) reflected by a decrease of microhardness and resistivity. At higher temperatures the β" phase is transformed into β_1 phase with fcc structure. Plates (200–500 nm in diameter) of the β_1 phase were observed by TEM in the alloy annealed up to 330 °C. The formation of the β_1 phase is accompanied by appearance of a defect component with lifetime $\tau_2 = 256$ ps in PL spectra. Intensity of this component steeply increases with temperature up to a maximum at 340 °C, see Fig. 2a. Thus, new positron traps are created by formation of the β_1 phase precipitates. Positrons are most probably trapped at misfit defect at the precipitate-matrix interfaces. However positron trapping inside the precipitates can not be excluded as well. An increase of resistivity and a decrease of I_2 above 340 °C is due to dissolution of the β_1 phase particles. This behavior is postponed in the temperature range (390–450) °C by formation of the β phase (plate-shaped particles 2–3 μm in diameter). The precipitation of the β phase causes a slight hardening seen in Fig. 3a. Above 450 °C the β phase precipitates dissolve and the solid solution is restored.

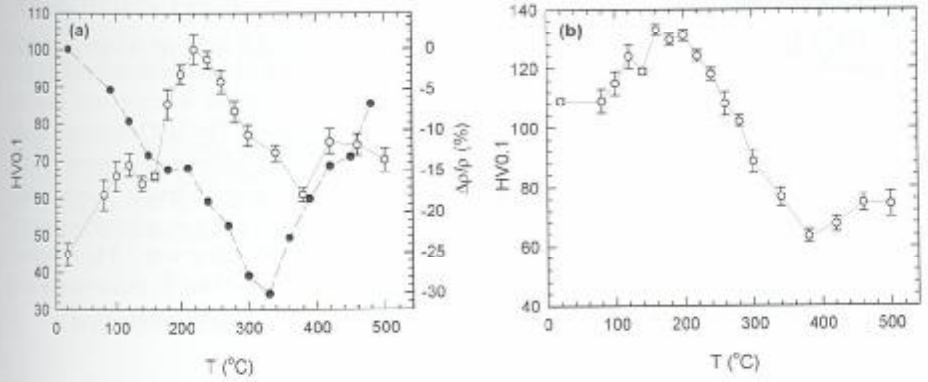

Figure 3: (a) solution treated Mg4Tb2Nd alloy – temperature dependence of microhardness (open circles) and the relative change of electrical resistivity (full circles); (b) HPT deformed Mg4Tb2Nd alloy – temperature dependence of microhardness

The microstructure development of HPT-deformed Mg4Tb2Nd includes not only the precipitation effects, but also the recovery of the defects introduced by SPD. The intensity I_2 of positrons trapped at dislocations exhibits an abrupt decrease in the temperature range (100–180) °C, see Fig. 2b. It gives a clear evidence for a recovery of dislocations which takes place in this temperature interval and was confirmed also by TEM (Fig. 1b). A single component PL spectrum above 180 °C indicates that the dislocation density dropped well below ≈ 10^{12}m^{-2}. The precipitation of the β" phase, which takes place at similar temperatures as in the coarse grained alloy, causes a remarkable hardening, see Fig. 3b. As has been already explained, PL spectroscopy is insensitive to the precipitation of the coherent β" phase. One can see in Fig. 2b that the intensity I_2 starts to increase again in the sample annealed up to 220 °C and exhibits maximum at 260 °C. The recovery of dislocations was completed already at 180 °C. Hence, this increase of I_2 is not connected with dislocations, but occurs due to positron trapping at defects introduced by precipitation of the β_1 phase particles. The lifetime of the defect component which appeared above 220 °C lies again around 256 ps. It supports the picture that this component comes from positrons trapped at the misfit defects at the β_1 phase incoherent interfaces. Precipitation of the β_1 phase is reflected also by an increase of microhardness. After annealing above 260 °C, the behavior of I_2 is reversed and it gradually decreases in similar manner as in the coarse grained alloy. The difference between the HPT-deformed and the coarse grained alloy consists in the fact that precipitation of the β_1 phase starts not at about 270 °C but already at 220 °C. As a consequence, the maximum of I_2 and the peak hardness in the HPT-deformed alloy are shifted to about of 80°C lower temperatures compared to the coarse grained alloy. Thus, the precipitation of the β_1 phase and most probably also the shape transformation of the β" phase start at significantly lower temperature in the HPT-deformed alloy. It has two reasons: (i) The extremely small grain size leads to a significant volume fraction of grain boundaries. The defects in grain boundaries serve as centers for nucleation of the second phase particles. (ii) Diffusivity of the Tb and Nd atoms is enhanced by a possibility to diffuse along grain boundaries. Both the factors facilitate the precipitation effects in the HPT-deformed alloy and shift the precipitation of the β_1 phase to lower temperatures.

4 Conclusions

The capability of HPT to achieve an extreme grain size refinement of was demonstrated in the present work on Mg4Tb2Nd alloy. The HPT-deformed alloy exhibits a grain size around 100 nm and a high density of homogeneously distributed dislocations. The UFG structure leads to a significant rise of hardness of the HPT-deformed alloy. Temperature development of microstructure of the HPT-deformed alloy was studied and compared with the coarse grained sample. Full recovery of dislocations in the HPT-deformed alloy takes place in relatively narrow temperature interval (100–180) °C. The precipitation sequence in the alloy with UFG structure differs from that in the coarse grained alloy. Namely the precipitation of the β_1 phase starts and shape transformation of the β'' phase take place at remarkably lower temperatures.

5 Acknowledgements

This work was financially supported by the Czech Science Foundation (contract 106/05/0073), The Ministry of Education, Youth and Sports of Czech Republics (project MS 0021620834), and INTAS.

6 References

[1] Mordike, B.L., Mat. Sci. Eng. A **2002**, *324*, 103–112.
[2] Neubert, V., Stulikova I., Smola, B., Mordike B.L., Vlach, M., Bakkar, A., Pelcova J., in: Proc. of ISPMA 10, Prague, September 2005, to be published in Mater.Sci. Eng. A.
[3] Valiev, R.Z., Islamgaliev, R.K., Alexandrov, I.V., Prog. Mat. Sci. **2000**, *45*, 103.
[4] Cizek, J., Prochazka, I., Stulikova, I., Smola, B., Kuzel, R., Cherkaska, V., Islamgaliev, R.K., Kulyasova, O., in: *Magnesium. Proceedings of the 6th International Conference Magnesium Alloys and Their Applications*, K.U. Kainer (Ed.), Wiley-VCH Weinheim **2003**, p. 202–207.
[5] Hautojärvi, P., Corbel, C., in: *Proceedings of the International School of Physics „Enrico Fermi"*, A. Dupasquier, A.P. Mills (Eds.), Course CXXV, IOS Press, Varena, **1995**, p. 491–562.
[6] Stulikova, I., Smola, B., Zaludova, N., Vlach, M., Pelcova, J., Kovove Mater. **2005**, *43*, 272–279.
[7] Becvar, F., Cizek, J., Lestak, L., Novotny, I., Prochazka, I., Sebesta, F., Nucl. Instr. Meth. A **2000**, *443*, 557–577.
[8] Cizek, J., Prochazka, I., Becvar, F., Stulikova, I., Smola, B., Kužel, R., Cherkaska, V., Islamgaliev, R.K, Kulyasova, O., phys. stat. sol. (a) **2006**, *203*, 466–477.
[9] Abdelrahman, M., Badawi, P., Jpn. J. Appl. Phys. **1996**, *35*, 4728–4729.